Extended Abstracts of the 2003 International Conference on Solid State Devices and Materials, Tokyo, 2003, pp. 76-77

D-1-6

Valence-Mended Si(100) for Nanoelectronic Applications

M. Tao, W. P. Kirk, D. Udeshi, S. Agarwal, E. Maldonado, and N. Basit

Department of Electrical Engineering and NanoFAB Center
University of Texas at Arlington, Arlington, TX 76019 USA
Phone: 817-272-5001; Fax: 817-272-7458; Email: mtao@uta.edu

1. Introduction

Dangling bonds are an inherent feature of a semiconductor surface. They make the surface behave significantly different from the bulk semiconductor. Surface states originate from dangling bonds. In chemical reactions, dangling bonds act as reaction sites. Figure 1(a) shows the atomic structure of a clean Si(100) surface in ultrahigh vacuum. Each surface atom possesses a dangling bond and shares a dimer bond with a neighboring surface atom. Both dimer bonds and back bonds are strained on this Si(100) surface, so they are chemically and electrically more active than the unstrained bonds in the bulk.

In this paper, we report a method to eliminate dangling bonds and strained bonds, and thus surface states, on Si(100) with a monolayer of 'valence-mending' atoms [1,2]. As shown in Fig. 1(b), a monolayer of Group-VI atoms can bridge between surface Si atoms and nicely eliminate dangling bonds and strained bonds on Si(100).

2. Results and Discussion

Table I lists our simulation results on bond lengths and interbond angles for O, S, and Se on Si(100). Se is the best choice for passivating Si(100) because it introduces the least strain. Table II lists our simulation results on surface energy of Si(100) with different passivation schemes. All Group-VI passivated surfaces have lower energy than H-passivated Si(100). Therefore, Group-VI passivated Si(100) surfaces should be thermally and chemically more stable than H-passivated Si(100).

Se passivation of Si(100) has been demonstrated using MBE techniques. Monolayer passivation is verified by RHEED and RGA. As shown in Fig. 2, RGA detects no Se for ~60 s after the Se shutter is opened, indicating that Se is initially adsorbed by the Si(100) surface. After the surface is covered with a monolayer of Se, excess Se is no longer adsorbed so it is bounced back from the surface and picked up by RGA. The desorption temperature of Se from Si(100) is determined by RHEED at ~710°C, as shown in Fig. 3. The desorption temperature of H from Si(100) is ~500 ºC [3]. Therefore, Se passivation can withstand much higher temperatures than H passivation.

Electrically, the Se passivation layer is only ~1 Å thick, so the Se-passivated Si(100) surface behaves just like a Si(100) surface but without surface states. Figure 4 shows activation-energy measurements of Al contacts on Se-passivated n-type Si(100). The Schottky barrier height is determined at 0.08 eV, which is significantly different from the barrier height reported in the literature, 0.72 eV [4]. The difference is attributed to the elimination of surface states on Si(100). The barrier heights of other metals on Se-passivated n-type Si(100) have also been determined, and they are all quite different from the data in the literature.

Figure 5 shows the I-V characteristics of Ti contacts on both bare and Se-passivated n-type Si(100). Both behave ohmically. Since the Si wafers have n-type doping in the low 10^{15} cm^{-3}, the ohmic behavior is believed to arise from the band diagram in Fig. 6. The key feature of this band diagram is its negative Schottky barrier, which promises an extremely-low internal resistance as compared to the current approach to ohmic contacts. When the two types of ohmic contacts undergo annealing, they turn from ohmic to Schottky but at different temperatures. As shown in Fig. 7, Se-passivated samples show thermally-stable ohmic behavior up to 425 °C, 200 °C more stable than bare samples. This thermal stability is important in device fabrication, and is attributed to the low surface energy of Se-passivated Si(100) (Table II).

3. Conclusions

The valence-mended Si(100) surface shows unprecedented structural, electrical, and chemical properties.

Acknowledgment

We would like to thank SRC for partial support of this research.

References

[1] E. Kaxiras, Phys. Rev. B43, 6824 (1991).
[2] M. Tao, D. Udeshi, N. Basit, E. Maldonado, and W.P. Kirk, Appl. Phys. Lett. 82, 1559 (2003).
[3] K. Sinniah, M.G. Sherman, L.B. Lewis, W.H. Weinberg, J.T. Yates, and K.C. Janda, J. Chem. Phys. 92, 5700 (1990).
[4] A.M. Cowley and S.M. Sze, J. Appl. Phys. 36, 3212 (1965).

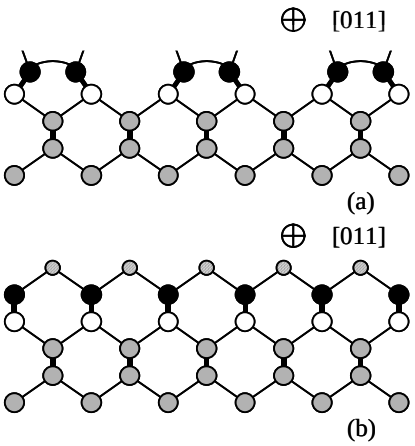

Fig. 1. Atomic structures of (a) reconstructed Si(100) surface and (b) Group-VI passivated Si(100) surface.

Table II. Surface energy of different Si(100) surfaces.

Surface	Energy (J/cm^2)
Clean Si(100) 2×1	0
Si(100) 2×1:H	-3.37×10^{-4}
Si(100) 1×1:Te	-8.34×10^{-4}
Si(100) 1×1:Se	-1.05×10^{-3}
Si(100) 1×1:S	-1.22×10^{-3}

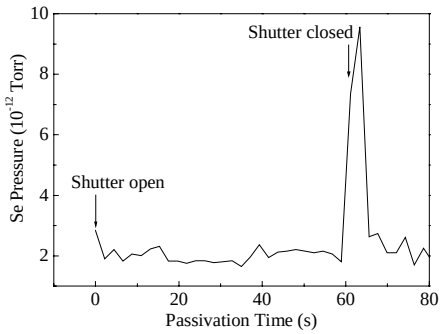

Fig. 2. Detection of Se bounced off the Si wafer by RGA.

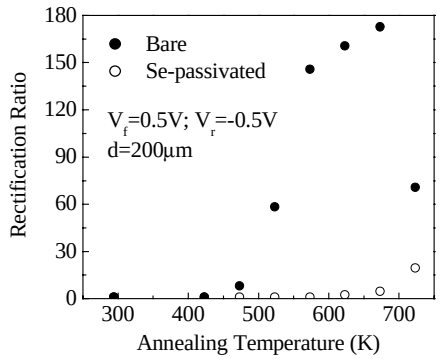

Fig. 7. Thermal stability of Ti-Si contacts upon annealing.

Table I. Bond lengths and interbond angles of Group-VI atoms on Si(100).

Element	O	S	Se	Te
a_o (Å)	1.51	1.93	2.06	?
a (Å)	1.98	2.01	2.06	
Δa (%)	31	4.1	0.0	
θ	153°	146°	138°	
Δθ	43.4°	36.7°	28.5°	

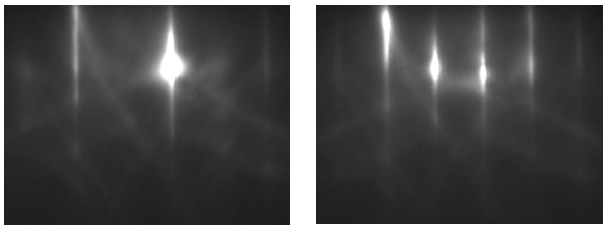

Fig. 3. RHEED patterns of Se-passivated Si(100) upon annealing. (a) 700°C and (b) 750°C.

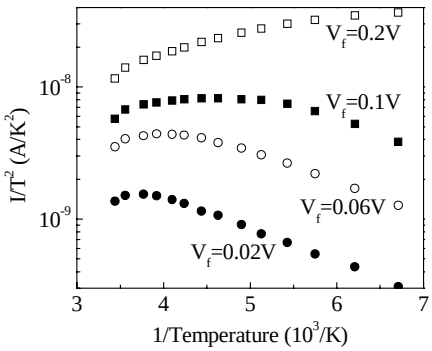

Fig. 4. Barrier height between Al and Se-passivated n-type Si(100) by the activation-energy method.

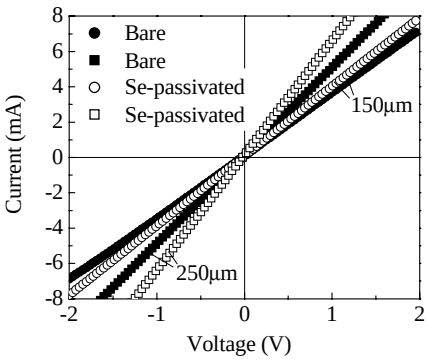

Fig. 5. I-V characteristics of Ti contacts on bare and Se-passivated n-type Si(100) with different dot sizes.

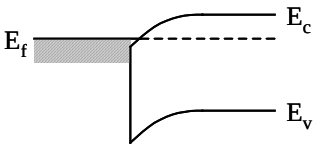

Fig. 6. Band diagram for a new approach to ohmic contacts.